Inorg. Chem. **2008**, *47*, 392–394

Facile Synthesis of Troilite

Nathalie M. Pedoussaut and Cora Lind*

Department of Chemistry, MS 602, The University of Toledo, Toledo, Ohio 43606

Received August 17, 2007

Low-temperature synthetic pathways can result in crystallization of metastable materials. These methods have been widely explored for the preparation of metal oxides. Adaptation of nonhydrolytic sol–gel chemistry to non-oxide systems offers an elegant route to transition-metal sulfides. The method can be exploited for the facile and reproducible synthesis of iron sulfide crystallizing in the troilite structure. This phase is only found in meteorites and planets and has previously been obtained by high-temperature or high-energy ball-milling methods. "Nonhydrolytic" sol–gel processing results in direct crystallization of troilite with no need for further calcination.

Troilite is the end member of the pyrrhotite family $Fe_{1-x}S$.[1] It has been found in meteorites, the Moon, and Mars[2−4] and has been identified as a stoichiometric to near-stoichiometric iron sulfide, crystallizing in the $P\bar{6}2c$ space group.[1−3] The crystal symmetry of pyrrhotites and troilites is based on NiAs superstructures. Troilite can be described as a 2C NiAs superstructure, with hexagonal lattice parameters $a = (\sqrt{3})$-a_{NiAs} and $c = 2c_{NiAs}$. This structure is stable below 140 °C and converts to a simple NiAs structure at higher temperatures. Its behavior as a function of pressure and temperature has been thoroughly investigated because it is of interest to geologists and space scientists for reconstructing the pressure/temperature history of meteorites and planets.[4] It is also the main sulfur-containing compound of the Moon's regolith, and its properties have been studied by NASA for in situ resource utilization. To avoid complications with respect to human health and the performance of equipment used, it is important to understand the impact of troilite on these factors. Synthetic troilite could be used for simulations of lunar regolith. This material can be prepared from its constituent elements by high-energy mechanical milling and by high-temperature techniques in evacuated quartz tubes. A problem encountered with these methods is to obtain homogeneous samples with reproducible stoichiometry, unless long heating times at high temperatures are used.[5−7]

Scheme 1. Formation of Iron Sulfide via a "Nonhydrolytic" Sol−Gel Reaction

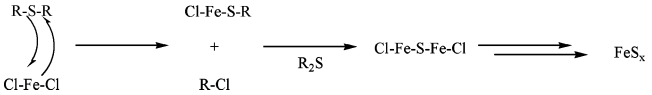

Low-temperature "chimie douce" routes to oxides are well explored, and application to non-oxide systems has grown over the last decades.[8,9] Among these soft chemistry techniques, nonhydrolytic sol−gel chemistry offers an elegant route to metal oxides and has been successfully applied to the preparation of stable and metastable compounds.[10] A similar reaction between metal halides and thioethers was briefly explored by Schleich's group in the 1980s but has received no attention since this time.[11] In this paper, we report a facile and reproducible low-temperature synthesis of troilite through the adaptation of a "nonhydrolytic" sol−gel process.

All steps were carried out under an inert atmosphere. In a typical synthesis, 3 mmol of $FeCl_2$, 11 mmol of *t*-Bu_2S, and 15 mL of dry CH_3CN were mixed in an ampule. The ampule was capped with a septum, transferred to a vacuum/inert gas manifold, cooled in liquid nitrogen, evacuated, and sealed. It was heated in a preheated oven at 130 °C for 7 days. The resulting powder was recovered by filtration with a yield of ∼30%. Heat treatments were carried out in a tube furnace under argon flow-through. Scheme 1 illustrates the reaction that leads to the formation of FeS_x.

Powder X-ray diffraction (XRD) data were collected on a Scintag XDS 2000 diffractometer in Bragg−Brentano geometry using Cu Kα radiation and a Moxtek solid-state detector. Phase identification was carried out using the *JADE*[12] software package and the ICDD PDF-2 database.

* To whom correspondence should be addressed. E-mail: cora.lind@utoledo.edu.

(1) Kissin, S. A.; Scott, S. D. *Econ. Geol.* **1982**, *77*, 1739−1754.
(2) Evans, J.; Howard, T. *Science* **1970**, *167*, 621−623.
(3) Howard, T.; Evans, J. *Proc. Apollo 11 Lunar Sci. Conf.* **1970**, *1*, 399−408.
(4) Fei, Y. W.; Prewitt, C. T.; Mao, H. K.; Bertka, C. M. *Science* **1995**, *268*, 1892−1894.
(5) Balaz, P.; Alacova, A.; Godocikova, E.; Kovac, J.; Skorvanek, I.; Jiang, J. Z. *Czech. J. Phys.* **2004**, *54*, D197−D200.
(6) Chin, P. P.; Ding, J.; Yi, J. B.; Liu, B. H. *J. Alloys Compd.* **2005**, *390*, 255−260.
(7) Schwarz, E. J.; Vaughan, D. J. *J. Geomagn. Geoelec.* **1972**, *24*, 441−458.
(8) Schleich, D. M. *Solid State Ionics* **1994**, *70/71*, 407−411.
(9) Gopalakrishnan, J. *Chem. Mater.* **1995**, *7*, 1265−1275.
(10) Andrianainarivelo, M.; Corriu, R. J. P.; Leclercq, D. *J. Mater. Chem.* **1997**, *7*, 179−284.
(11) Martin, M. J.; Qiang, G. H.; Schleich, D. M. *Inorg. Chem.* **1988**.
(12) *JADE*; Materials Data Inc.: Livermore, CA. www.MaterialsData.com.

10.1021/ic701636h CCC: $40.75
Published on Web 12/23/2007

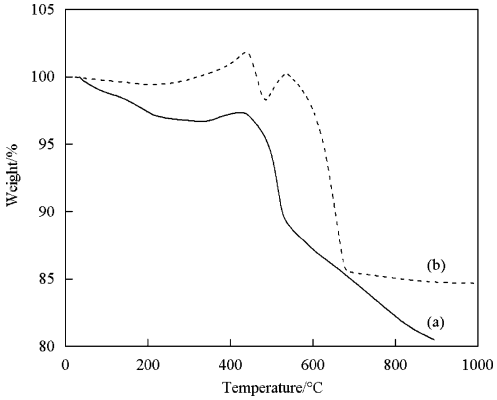

Figure 1. TGA data for an Fe_xS sample upon heating under (a) nitrogen and (b) air.

Rietveld refinements in *FullProf*[13] were used to confirm the structure of the samples. CHN analyses were carried out on a Perkin-Elmer series II 2400 analyzer. The sample composition was also studied by thermogravimetric analysis/differential thermal analysis (TGA/DTA) on a TA Instruments SDT 2960 DTA−TGA and by energy-dispersive X-ray spectroscopy (EDS) on a Hitachi S-2400 scanning electron microscope. The EDS analysis was semiquantitative.

XRD analysis showed that the as-recovered powders were crystalline. The patterns of all samples displayed sharp peaks that matched well with the PDF card for troilite (89-6927). The raw samples also contained a small amount of greigite (Fe_3S_4), which could be removed by heating to 500 °C for 5 h under argon in a tube furnace.

The completeness of the reaction was investigated by CHN analysis. The raw samples contained less than 1.5% of carbon, indicating almost complete reaction. This agreed well with TGA data, which showed only a few percent of weight loss at low temperatures upon heating in nitrogen (Figure 1). The samples also appeared to contain some volatile sulfur, as evidenced by a sharp mass loss around 450 °C. The decomposition of greigite could contribute to the observed loss. Continued heating resulted in a slower mass loss, which could correspond to the loss of structural sulfur. This is in agreement with previous studies, which reported that FeS decomposes to Fe and $Fe_{1-x}S$.[14]

The iron-to-sulfur ratio was determined by TGA in air. Experiments were carried out from room temperature to 900 °C to oxidize the sample to Fe_2O_3. In order to get an estimate of the structural sulfur only, the sample was preheated to 450 °C for 10 min under nitrogen to evaporate any unreacted sulfur. The data collected in air showed an exothermic event and a gain of mass, as $FeSO_4$ was formed, followed by a loss of mass, due to the final oxidation to Fe_2O_3 (Figure 1). The powder recovered after this run was analyzed by XRD, which confirmed the presence of Fe_2O_3. Assuming an initial stoichiometry of Fe_xS, values of $x = 0.93-0.95$ were determined. However, it was impossible for this procedure to judge whether all excess sulfur had been evaporated. To overcome this problem, several samples were heated for 5 h in a tube furnace at 500 °C under argon. The samples were characterized by XRD before TGA analysis. This gave Fe_xS compositions with x between 0.85 and 0.88, indicating that not all unbound sulfur may have been evaporated in the original TGA experiments. The loss of greigite could also contribute to the lower overall iron-to-sulfur ratio observed for the preheated samples.

EDS analysis gave elemental compositions of $Fe_{0.84}S$ to $Fe_{0.91}$ for all samples. For unheated samples, greigite particles with compositions of $Fe_{0.72}S$ to $Fe_{0.78}S$ were also detected. No significant changes in the EDS composition were observed for heat-treated samples. Some variation was observed between individual particles, resulting in standard deviations of 3−9% for most samples.

The iron-to-sulfur ratios determined by TGA and EDS were lower than generally accepted compositions for troilite ($x = 0.95-1$),[15−17] suggesting that the samples might be hexagonal or monoclinic iron-deficient pyrrhotites. However, troilites with lower iron contents than 0.95 have been reported previously.[1,18,19] The phase diagram at room temperature is not well-defined for Fe_xS compositions with values of $0.85 < x < 0.95$.[1] To confirm the identity of our samples, high-quality XRD data were collected on a sample. The elemental composition of this sample was $Fe_{0.93}S$ by TGA and $Fe_{0.91}S$ by EDS. The stoichiometry can also be estimated from the d spacing of the 102 reflection in the corresponding NiAs structure using the following equation:[14,19]

$$Y = 45.212 + 72.86(d_{102} - 2.0400) + 311.5(d_{102} - 2.0400)^2$$

where Y is the atomic percentage of Fe and d_{102} is given in angstroms. This gives a composition of $Fe_{0.88}S$, which is equivalent to Fe_7S_8. Iron sulfides with this composition generally crystallize in the monoclinic 4C pyrrhotite structure. The diffraction data were subjected to peak-width analysis to address whether the sample adopted a monoclinic or hexagonal structure. For the unheated samples, the highest peak at ∼44° 2θ had a full width at half-maximum (fwhm) that was comparable to that of other peaks (∼0.20−0.25°). This peak is expected to be a single peak for troilite, while two overlapping reflections contribute to this peak in monoclinic Fe_7S_8. In contrast, for the samples treated to 500 °C, the fwhm almost doubled, while the widths of other peaks remained similar. This suggests that the samples undergo an irreversible phase transition to the monoclinic Fe_7S_8 polymorph. During an in situ variable-temperature diffraction study, broadening of the 44° peak was observed starting at 250 °C. At the same temperature, a new peak at around 35° is observed in the pattern. This reflection is predicted to have no intensity in the troilite structure but should be observed in monoclinic Fe_7S_8. In addition, forma-

(13) Rodriguez-Carvajal, J. *Satellite Meeting on Powder Diffraction of the XV Congress of the IUCr*, Toulouse, France, 1990; p 127.
(14) Selivanov, E. N.; Vershinin, A. D.; Gulyaeva, R. I. *Inorg. Mater.* **2003**, *39*, 1097−1102.
(15) Kellerbesrest, F.; Collin, G. *J. Solid State Chem.* **1990**, *84*, 194−210.
(16) Li, F.; Franzen, H. F. *J. Alloys Compd.* **1996**, *238*, 73−80.
(17) Wang, H. P.; Salveson, I. *Phase Trans.* **2005**, *78*, 547−567.
(18) Jiang, J. Z.; Larsen, R. K.; Lin, R.; Morup, S.; Chorkendorff, I.; Nielsen, K.; Hansen, K.; West, K. *J. Solid State Chem.* **1998**, *138*, 114−125.
(19) Yund, R. A. *Econ. Geol. Bull. Soc. Econ. Geol.* **1969**, *64*, 420−423.

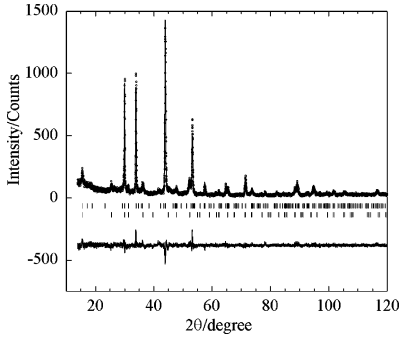

Figure 2. Rietveld refinement of Fe_xS using the troilite structural model. Circles represent data points, the calculated pattern corresponds to the solid line, and a difference plot is shown below the pattern. Tick marks indicate calculated peak positions for troilite (top trace) and greigite (lower trace).

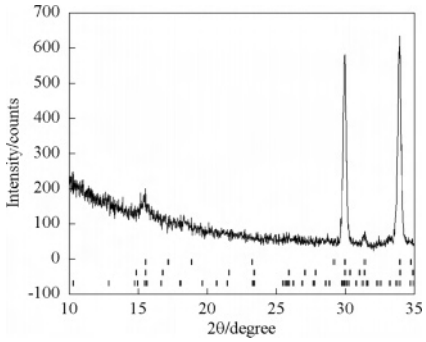

Figure 3. Low-angle region of the XRD pattern with tick marks for expected superlattice peak positions for troilite (top), 4C pyrrhotite (middle), and 6C pyrrhotite (bottom).

tion of pyrite was observed during the in situ study starting at 250 °C. The peak width of the 44° reflection decreased above 350 °C, corresponding to the transformation of Fe_7S_8 to a simple, hexagonal NiAs structure. This transition was accompanied by the formation of more pyrite. Peaks corresponding to the initially observed greigite phase, Fe_3S_4, disappeared between 300 and 350 °C. An ex situ study, during which the sample was consecutively heated to temperatures between 100 and 500 °C in 50 °C intervals with 4 h holding times at each temperature, showed the formation of pyrite and the disappearance of greigite at the same temperatures as those in the in situ study. No pyrite was observed in the samples treated to 450 and 500 °C. In addition, the fwhm of the 44° peak increased with temperature even above 350 °C, indicating that a monoclinic pyrrhotite was recovered at room temperature. These two studies agree well with the phase diagram for Fe_7S_8, which predicts crystallization of pyrite and loss of sulfur from the monoclinic phase above 210 °C, followed by transformation of monoclinic Fe_xS to a mixture of NiAs-type FeS and FeS_2 above 310 °C.[1] At higher temperatures, more sulfur-rich compositions become thermodynamically favorable again, which could explain the formation of single-phase pyrrhotite above 450 °C. Single-phase pyrrhotite samples recovered from 500 °C heat treatments showed the presence of pyrite in the pattern after an additional heat treatment at 300 °C.

Table 1. Refinement Results for Fe_xS Prepared by Nonhydrolytic Sol−Gel Chemistry for Troilite and Several Pyrrhotite Structures

structure	formula	space group	R_{Bragg}	χ^2
		Structural Fit		
NiAs	$Fe_{1-x}S$	$P\bar{6}_3/mmc$	7.3	1.7
troilite	$Fe_{1-x}S$	$P\bar{6}2c$	7.3	1.6
4C, 3T	Fe_7S_8	$P3_121$	14.8	1.9
4C	Fe_7S_8	$C2/c$	16.3	2.4
		Le Bail Fit		
NiAs	$Fe_{1-x}S$	$P\bar{6}_3/mmc$	4.13	1.5
troilite	$Fe_{1-x}S$	$P\bar{6}2c$	0.89	1.4
4C	Fe_7S_8	$P6mcc$	0.94	1.4
4C	Fe_7S_8	$C2/c$	1.56	1.7
4C, 3T	Fe_7S_8	$P3_121$	1.56	1.4
5C	Fe_9S_{10}	$P6$	1.79	1.3
6C	$Fe_{11}S_{12}$	$P6$	1.02	1.4

To further investigate whether the unheated samples possessed the troilite structure with a composition that should adopt the monoclinic Fe_7S_8 structure, the X-ray data were refined for several superstructures corresponding to troilite and different pyrrhotites. Crystal structure models are available for NiAs, troilite,[2,3] and Fe_7S_8 (4C pyrrhotite, monoclinic and hexagonal structures).[20] Rietveld refinements were carried out for all models. A significantly better fit was obtained for the troilite structure (Figure 2 and Table 1). The simple NiAs structure does not account for several small peaks. Because no structural models are available for a number of pyrrhotite unit cells, Le Bail fits were carried out for all commensurate hexagonal unit cells. The results are summarized in Table 1. The best refinement statistics were obtained for troilite ($R_{Bragg} = 0.89\%$; $\chi^2 = 1.4$), 4C pyrrhotite ($R_{Bragg} = 0.94\%$; $\chi^2 = 1.4$), and 6C pyrrhotite ($R_{Bragg} = 1.02\%$; $\chi^2 = 1.4$). The fact that troilite, refined in a higher symmetry space group and with smaller lattice constants, gives a comparable fit to the 4C and 6C pyrrhotites suggests that the sample is, in fact, composed of troilite. In addition, the presence of a considerable number of superlattice reflections would be expected in the X-ray pattern. A very slow scan of the low-angle region only showed the presence of superlattice reflections corresponding to the troilite unit cell (Figure 3), confirming that the sample is made of troilite. The lattice parameters from Rietveld analysis were $a = 5.9668$ Å and $c = 11.4027$ Å, and the elemental composition was refined to $Fe_{0.92}S$.

In conclusion, we have extended the application of nonhydrolytic sol−gel chemistry to the synthesis of transition-metal sulfides. This process provides a facile and reproducible route to Fe_xS with the troilite structure. The method can stabilize the 2C superstructure for iron-deficient compositions. An irreversible transformation to monoclinic pyrrhotite occurs above 250 °C. Our approach is well suited for the preparation of troilite for simulations of lunar regolith, which could be of importance for future space missions.

Acknowledgment. The authors thank Kenneth W. Street for helpful discussions.

IC701636H

(20) Nakano, A. *Acta Crystallogr., Sect. B* **1976**, *B35*, 722−724.